CHIMIA 51 (1997) Nr. 10 (Oktober)

Chimia 51 (1997) 760–767

ISSN 0009–4293

Optical Microscopy in the Nano-World

Dieter W. Pohl[a]*, **Hermann Bach**[b], **Martin A. Bopp**[c], **Volker Deckert**[d], **Pierre Descouts**[e], **Rolf Eckert**[c], **Hans-Joachim Güntherodt**[c], **Christian Hafner**[f], **Bert Hecht**[b], **Harry Heinzelmann**[c], **Thomas Huser** [c], **Mark Jobin**[e]**, **Ursula Keller**[g], **Thilo Lacoste**[c], **Patrick Lambelet**[h], **Fabienne Marquis-Weible**[h], **Olivier J.F. Martin**[f], **Alfred J. Meixner**[c], **Bettina Nechay**[g], **Lukas Novotny**[f], **Michael Pfeiffer**[h], **Claude Philipona**[h], **Taras Plakhotnik**[b], **Alois Renn**[b], **Abdeljalil Sayah**[h], **Joao-Manuel Segura**[b], **Beate Sick**[b], **Uwe Siegner**[g], **Guido Tarrach**[c], **Rüdiger Vahldieck**[f], **Urs P. Wild**[b], **Dieter Zeisel**[d], and **Renato Zenobi**[d])

Abstract. Scanning near-field optical microscopy (SNOM) is an optical microscopy whose resolution is not bound to the diffraction limit. It provides chemical information based upon spectral, polarization and/or fluorescence contrast images. Details as small as 20 nm can be recognized. Photophysical and photochemical effects can be studied with SNOM on a similar scale. This article reviews a good deal of the experimental and theoretical work on SNOM in Switzerland.

Introduction

Light microscopy, first demonstrated in the late 16th century, has long since matured into a standard technique in such diverse fields as biology, medicine, electronics, and materials sciences. The wealth of optical methods guarantees conventional light microscopy a place in the laboratory although the resolution limit of, say, 200–500 nm, imposed by the laws of diffraction, often is insufficient for modern characterization problems. Until recently, it was necessary to fall back upon electron, tunnel, or atomic force microscopies in such a situation. These techniques yield excellent images of the sample topography with resolution down to the atomic scale. However, their chemical specificity is in general low. The electron microscope, moreover, requires operation in vacuum, which can deteriorate the sample and complicates the inspection process. The microscopists' dream, therefore, was and is a microscope that combines the specificity and simplicity of optical characterization with the resolving power of an electron microscope. The recent developments in scanning near-field optical microscopy may be considered a first step towards the realization of this dream.

In optical imaging, the only way to achieve a resolution beyond the diffraction limit is light confinement by material probes. Such probes must be positioned in the immediate proximity of the sample surface, as confinement is restricted to distances comparable to the size of the probe. The confined field just behind an illuminated aperture, *e.g.*, is a hemisphere of roughly the same diameter as that of the aperture. The latter can be made much smaller than the optical wavelength. Similarly, the field enhancement next to a scattering particle decays over a distance that roughly equals its radius, hence can again be much smaller than the wavelength. Fields that decay over such small distances are called evanescent waves because they do not obey the usual laws of wave propagation although they are solutions of *Maxwell*'s wave equation.

For selective interaction, the probe is scanned in the immediate proximity of the sample surface. For this purpose, the aperture or scattering particle usually forms the apex of a pointed tip similar to the ones used in other scanning probe microscopies (*Fig. 1*). The confinement radius of the evanescent field and the distance between sample and probe determine the degree of overlap of the evanescent waves with the characteristic structures of the sample. This in turn determines the resolution of the scanning near-field optical microscope (SNOM). As a rule of thumb, the resolution in SNOM is limited by the larger of the two parameters. Typical practical values obtained for the light confinement structures are 20–80 nm.

Although proposed several times before in this century, this idea took until 1984 before it was converted into an operable microscope, a development that actually took its origin in Switzerland [2]. In the first experiments that used an aperture as probe, a 'super'-resolution of 20–50 nm was achieved in transmission [3][4], confirmed shortly afterwards by independ-

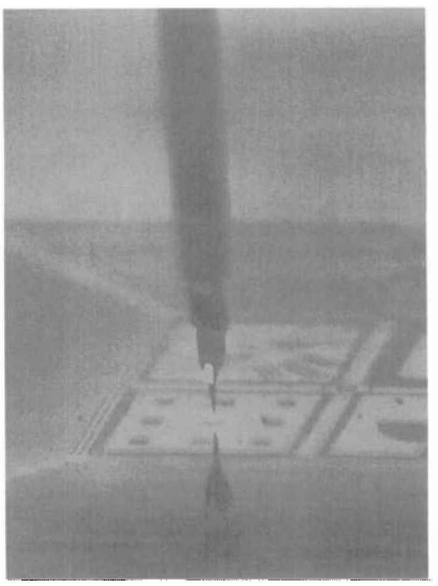

Fig. 1. *SNOM fiber probe approaching a test sample surface.* From [1].

*Correspondence: Dr. D.W. Pohl[a])
[a]) *IBM* Research Division
Zürich Research Laboratory
CH-8803 Rüschlikon
[b]) Laboratory of Physical Chemistry
Swiss Federal Institute of Technology
ETH-Zentrum
CH-8092 Zürich
[c]) Institute of Physics
University of Basel, Klingelbergstrasse 82
CH-4056 Basel
[d]) Laboratory of Organic Chemistry
Swiss Federal Institute of Technology
ETH-Zentrum
CH-8092 Zürich
[e]) Groupe de Physique Appliquée
Université de Genève
20, rue de l'Ecole-de-Medicine
CH-1211 Genève 4
** Present address:
Park Scientific Instruments SA, Genève
[f]) Laboratory of Field Theory and Microwave Electronics
Swiss Federal Institute of Technology
ETH-Zentrum
CH-8092 Zürich
[g]) Institute of Quantum Electronics
Swiss Federal Institute of Technology
ETH-Hönggerberg
CH-8092 Zürich
[h]) Laboratoire d'Optique Appliquée
Ecole Polytechnique Fédérale Ecublens
CH-1015 Lausanne

ently obtained results in the United States [5]. Reflection SNOM with similar resolution was demonstrated for the first time in 1988 [6]. The resolution routinely achieved nowadays still is of the same size; an improvement by one order of magnitude appears feasible, though.

Most of the work presented here is based on the usage of aperture SNOM (a-SNOM). The most popular types of these microscopes utilize optical fibers as probes. The probe end of the fiber is shaped into a pointed tip and coated with a metal film in such a way that a small area at the very apex is left uncoated, representing the aperture [7]. The light source typically is a laser, the radiation of which can be coupled conveniently into the far end of the light-guiding structure. The light transmitted by aperture and sample is collected by a classical optical microscope or by an appropriate focusing mirror and detected with a photomultiplier, an avalanche photodiode (APD), or a CCD camera. The detected light flux varies during scanning in accordance with the variation of the dielectric and topographic properties of the sample, resulting in scan images quite similar to classical optical micrographs but with higher resolution.

The probe/sample distance ('gap width') is controlled by piezo-electric actuators. An auxiliary sensor, usually based on the detection of frictional shear forces (SF) between the laterally vibrating probe tip and the sample surface, provides an approach signal. A control loop can regulate the piezo-electric actuator in such a way that the SF signal remains constant during scanning. In this mode of operation, the actuator voltage provides an image of the sample topography simultaneously with the optical image. This additional information can be very useful but the auxiliary control mechanism can also cause serious artifacts in a SNOM image ('z'-motion artifact). For critical SNOM applications, the sample, therefore, has to be scanned a second time at constant height, with the distance control turned off [8].

SNOM is most advantageously applied to surfaces for which material contrast with a resolution of 10–100 nm is of chief importance, *e.g.*, in biology or microelectronics. There are only few restrictions regarding the sample environment, allowing SNOM imaging in air, water, vacuum, or at extreme temperatures.

At dimensions of less than 100 nm, all the relevant interactions are of near-field optical (NFO) type. They cannot be described with the theoretical tools of classical optics but require the solution of *Maxwell*'s equations for the appropriate boundary conditions – a task that in most cases can only be solved numerically. Theoretical predictions about SNOM imaging properties, therefore, are difficult to achieve but might become instrumental for further improvement of resolution, image interpretation, and many applications.

In Switzerland, a number of research groups use SNOM and/or are working on

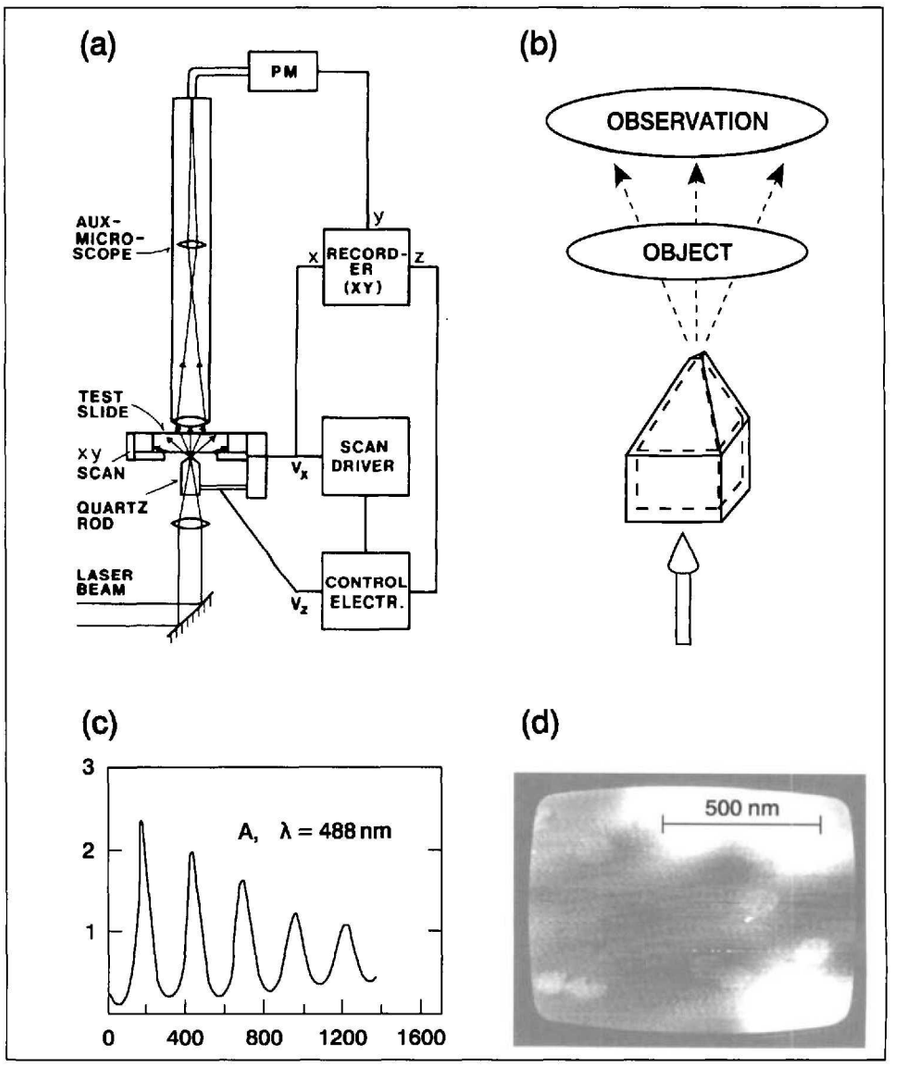

Fig. 2. *The original SNOM. a*) Setup, PM denotes the photomultiplier (from [2]), *b*) scheme of quartz probe tip, *c*) approach curves (horizontal: gap width in nm, vertical: far-field intensity, arbitrary units) (from [19]), and *d*) SNOM image of metal pattern allows details of *ca.* 20 nm in diameter to be recognized (from [3]).

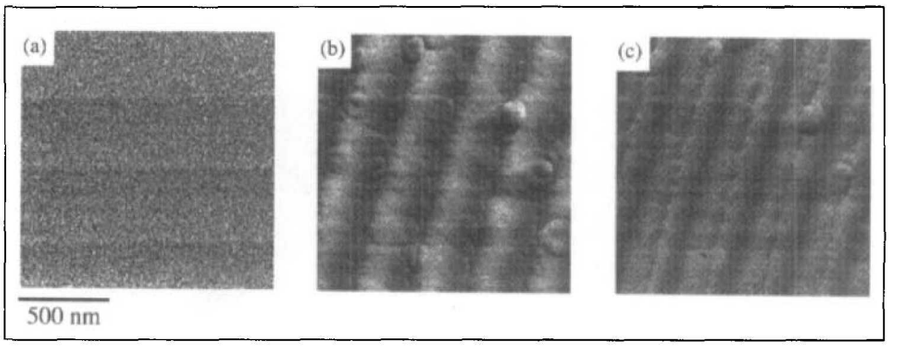

Fig. 3. *High-resolution NFO imaging of a glass grating* (courtesy *B. Curtis*, PSI Zürich) *with a period of 390 nm, a step height of 8 nm, in constant-height mode:* a) *constant voltage at piezo-electric actuator indicates that the probe did not touch the sample surface anywhere, although it was adjusted to scan in its immediate proximity;* b) *allowed and* c) *forbidden light images.* Details 10 nm in size can be recognized thanks to an exceptionally good aperture probe. From [8].

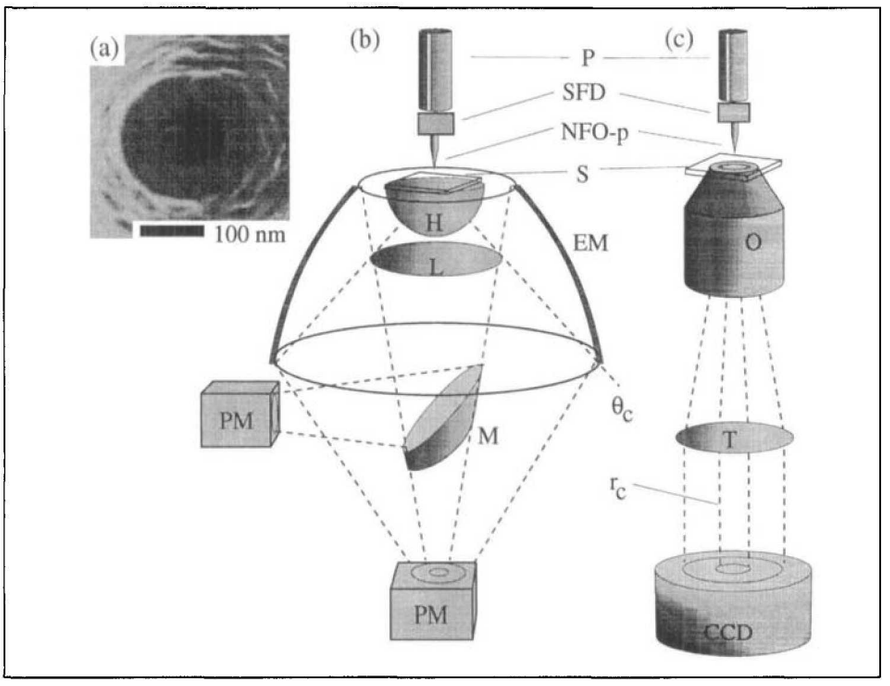

Fig. 4. a) *Scanning electron microscope image of the apex of a typical NFO fiber probe with aperture.* b, c) *TNOM setups, P: piezo-electric tube scanner, SFD; shear force detector, NFO-p: NFO probe, S: sample.* The detection optics is based on the combination of a hemispherical substrate (H) with an elliptical mirror (EM) in *b*) and on using an inverted optical microscope with an N.A. = 1.3 objective (O) in optical contact with S in *c*). The other letters denote; L, T: collection and tubus lens, respectively; M: mirror; PM: photomultiplier; CCD: CCD camera (for detection of spatial and angular distribution). From [20].

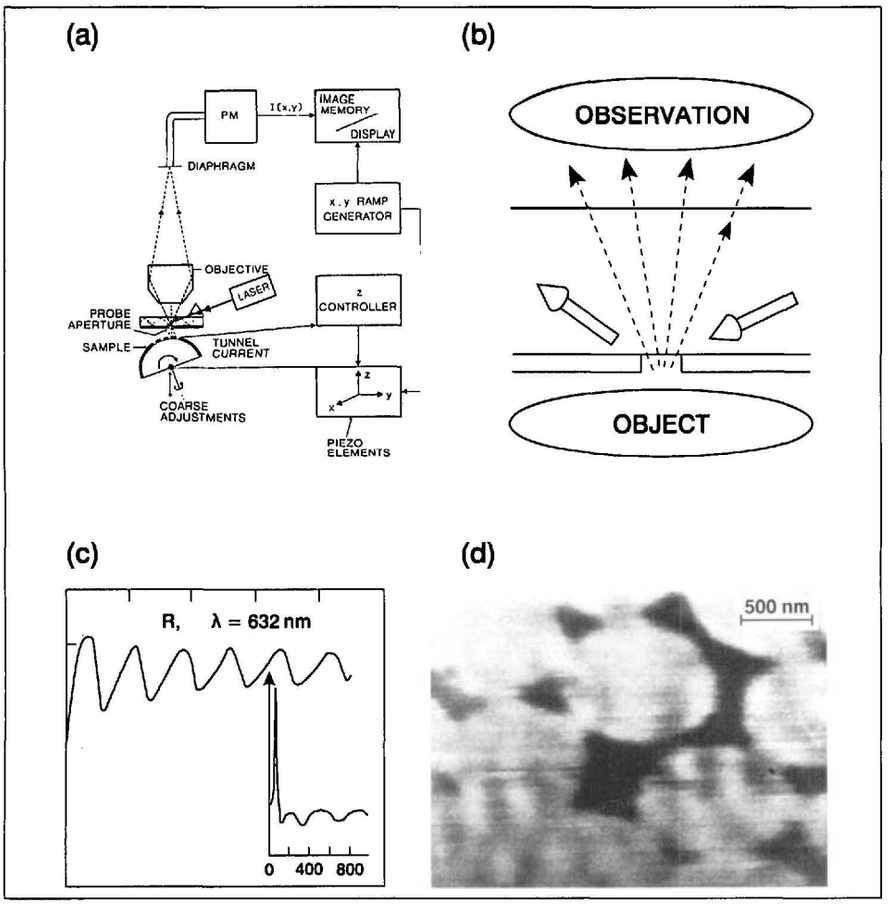

Fig. 5. a) *Reflection SNOM setup* (from [6]), b) *scheme of aperture dark-field arrangement,* c) *approach curves for reflection and plasmon excitation* (scales same as in *Fig. 2, c*), *adapted from* [19], *and* d) *image of metal pattern, from* [6]

SNOM problems. The present article briefly reviews the activities at the *IBM* Research Laboratory in Rüschlikon, at the Universities of Basel and Geneva, and at the Federal Institutes of Technology in Zürich (ETH) and Lausanne (EPFL).

The fields of research include both general studies in near-field optics and the application of SNOM to various problems in material science, chemistry, and biology. For these purposes a number of specialized different microscopes have been developed [9–17]. A SNOM that allows ultrafast spectroscopic techniques to be combined with high spatial resolution is under construction at the ETH [18]. In Geneva and Lausanne, the design of a SNOM particularly suitable for biological objects was started.

Near-Field Optics at *IBM* Rüschlikon

SNOM in Transmission

The nowadays popular aperture-SNOM is based on the original 'Swiss' design (*Fig. 2*) [2–4] developed at the *IBM* Research Laboratory in Rüschlikon in the years 1983–1985. As optical probe it employed a quartz crystal cut, polished, and etched in such a way that three facts formed an almost atomically sharp point. The crystal was coated completely with an opaque aluminum film except for the entrance face opposite the tip onto which a laser beam was focused (*Fig. 2, b*). The aperture was created by pressing the tip against the sample, causing plastic deformation of the coating until a faint emission of light from the tip could be detected. These optical probes had a large apex angle, which is essential for efficient light throughput, and extremely small apertures; indeed, the resolution achieved with these probes is unsurpassed in present-day routine NFO microscopy. Unfortunately, these probes were difficult to prepare and too short-lived for routine operation.

Fig. 2, d shows an image obtained with this type of SNOM. The object is a semi-transparent Ta film with holes of 100 nm diameter. The holes are shadow images of latex spheres randomly dispersed on the glass substrate during evaporation. They are clearly visible, together with even smaller details, for instance the ≈ 20-nm-wide peninsula protruding into the pair of holes near the lower right-hand corner. Note that the image is a simple screen shot, as digital image processing was not yet available to us at the time the image was made.

A 'modern' SNOM image of a phase object, indicating the high resolution

achievable, is shown in *Fig. 3*. It was obtained with an advanced version of an a-SNOM, sketched in *Fig. 4, b*. The NFO probe is an optical fiber, an end view of which is shown in *Fig. 4, a*. The black area in the center is the aperture. The grains of the aluminum coating are of similar size as the aperture. They cause irregularities in the aperture shape, which vary from probe to probe, a distinct shortcoming of the current probe-preparation technique. The fiber end sticks out from a piezo-electric tube scanner, *Fig. 4, b* and *c* (top), allowing lateral scanning as well as approach and distance regulation of the NFO probe (see *Sect.* 'Forbidden Light' SNOM).

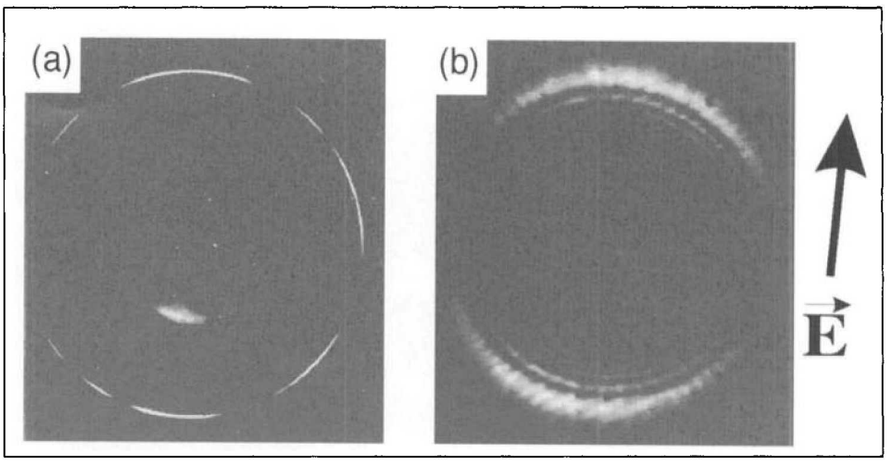

Fig. 6. *Angular distribution of transmitted radiation;* a) *silver film,* $\lambda = 514$ *nm, elliptic polarization;* b) *gold film,* $\lambda = 633$ *nm, linear polarization along* Ė. From [20].

SNOM in Reflection

The optical probe sketched in *Fig. 5, a* was developed for operation in reflection mode. The figure shows a section of a planar optical waveguide placed close to the sample surface. Light scattered by imperfections, such as the hole in *Fig. 5, b*, is the only light observed in the far field – it is essentially a dark-field scheme [6]. The scattering intensity in the upward direction depends on the proximity of the sample surface, *Fig. 5, c*. It is possible, in particular, to excite a localized plasmon if the aperture is replaced by a protrusion at a certain small gap width; under these conditions, the particle will show up brightly (narrow peak in the approach curve shown in the inset of *Fig. 5, c*) [21]. *Fig. 5, d* is an image obtained with the probe in *Fig. 5, b*. A drawback of the method is its restriction to planar or convex samples.

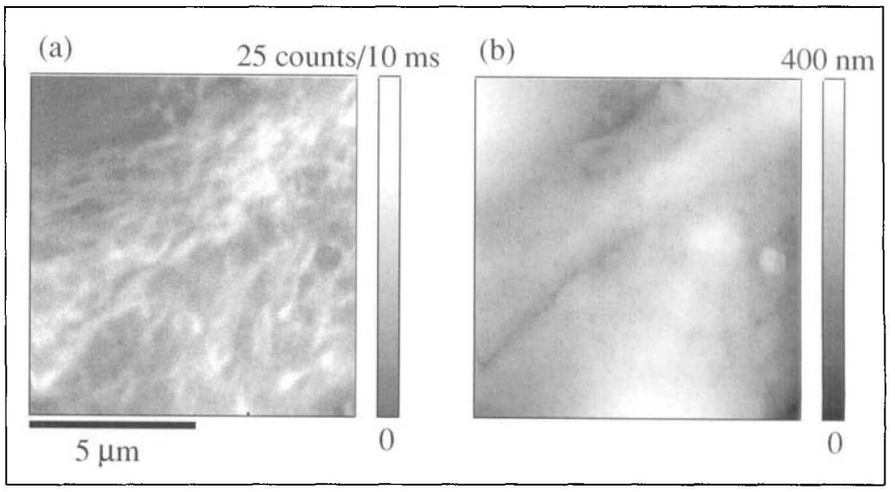

Fig. 7. *T3 fibroplast cell, cytoskeleton labeled with rhodamine-6G* (prepared at the University of Geneva)*: a) NFO fluorescence imaging, constant-gap-width mode, almost free of z-motion artifacts, and* b) *SF image.* Adapted from [8].

'Forbidden Light' SNOM

The SNOMs shown in *Fig. 4, b* and *c* are called tunnel SNOM (TNOM) because they can detect light coupled *via* evanescent waves (photon tunneling) into the object. This happens when the gap width is smaller than *ca.* one wavelength [9][10][15]. The respective contributions are transmitted at angles larger than the critical one and, therefore, are 'forbidden' for regular SNOM; they require an object carrier, *e.g.*, of hemispherical shape (*Fig. 4, b*) or in optical contact with an N.A. ≥ 1 objective (*Fig. 4, c*).

The gap-width-dependent transmission of 'forbidden' light provides distinctly different, frequently enhanced contrast when compared to the regular 'allowed' a-SNOM mode; moreover, it is suitable for optical gap-width regulation.

Local Excitation, Scattering, and Interference of Surface Plasmons

The optical probe of SNOM acts as a point source of surface plasmon (SP) polaritons on gold and silver films. Plasmon excitation manifests itself by emission of light in the direction of the SP resonance angle (*Fig. 6*), originating from an area shaped like a dipole radiation pattern whose extension is given by the SP decay length. Interaction with selected, individual surface inhomogeneities gives rise to characteristic modifications of the emitted radiation, which provide detailed information about SP scattering, reflection, and interference phenomena [20].

Artifacts in NFO Microscopy

NFO microscopes with an auxiliary gap-width regulation (shear force, tunneling) may produce images that represent the path of the probe rather than the optical properties of the sample. Experimental and theoretical evidence led us to the conclusion that many NFO results reported in the past may have been affected or even dominated by the resulting artifact ('*z*'-motion artifact). The specifications derived from such results for the various types of NFO microscopes used, therefore, warrant reexamination. The only modes of operation that reliably avoid the artifact are feedback control of the NFO signal (constant-intensity mode), but which is difficult to interpret, and scanning without feedback control (constant-height mode) [8].

Imaging Biological Specimen by Near-Field Optics at the University of Geneva and at EPFL

Fig. 7 depicts part of a T3 fibroplast cell, prepared and being studied at the University of Geneva, imaged at the *IBM* Zürich Research Laboratory. The actin cytoskeleton is labeled with a fluorescent dye. The shear-force topographic image shows the more or less smooth cell surface, whereas the NFO image clearly reveals the skeleton structure. The finest

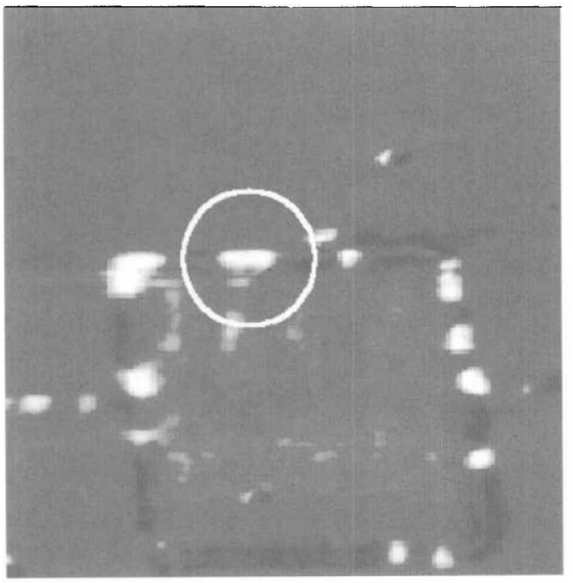

Fig. 8. *Polarization SNOM image of a thin liquid-crystal polymer film consisting of areas having different molecular orientation.* The resulting changes in birefringence are clearly visible in the image. The polarization of the illuminating light was kept constant during scanning. The size of the square is *ca.* 6 × 6 μm².

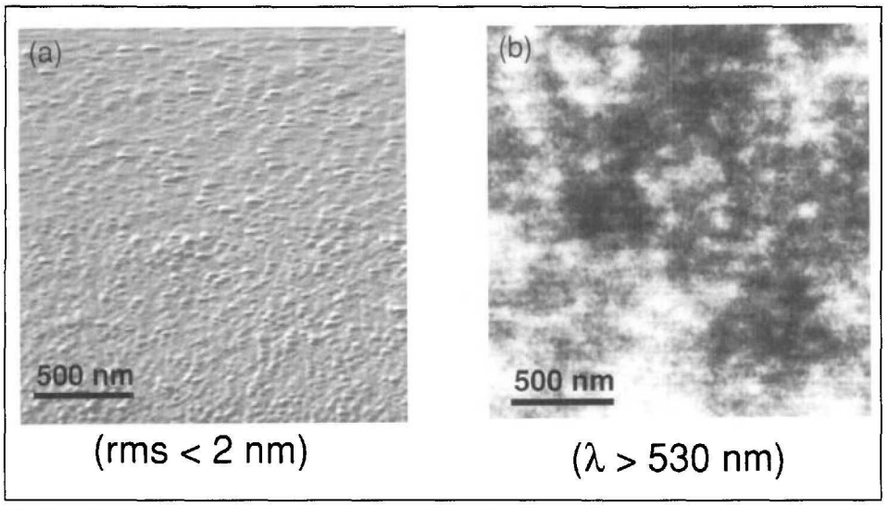

Fig. 9. a) *Surface topography and* b) *super-resolution fluorescence image of a glass slide onto which the dye rhodamine-6G was deposited at low concentration*

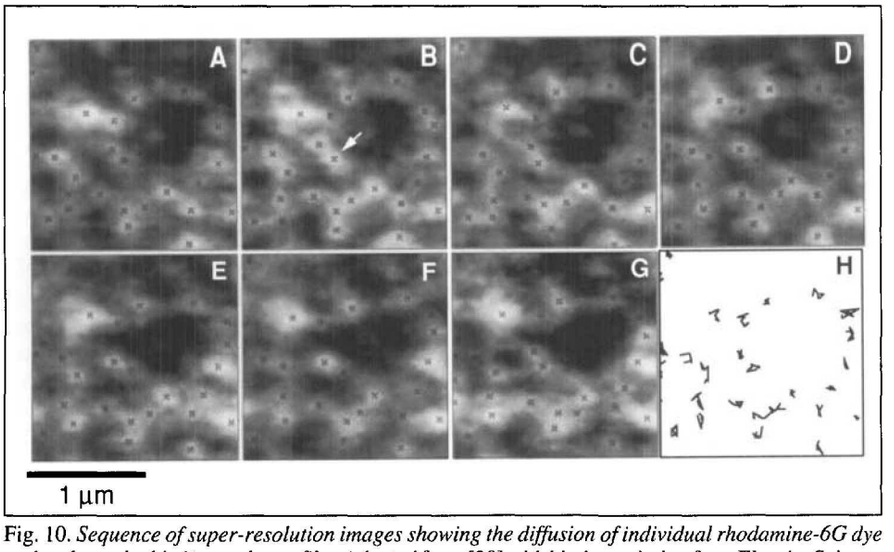

Fig. 10. *Sequence of super-resolution images showing the diffusion of individual rhodamine-6G dye molecules embedded in a polymer film.* Adapted from [30] with kind permission from Elsevier Science – NL, Sara Burgerhartstraat 25, NL–1055 KV Amsterdam.

recognizable details are 50–100 nm in size [8][15].

The SNOM group at the EPFL develops specific applications of near-field photochemical interactions with biomolecules. For this purpose, its research is currently focused on some key instrumental aspects [22] and the improvement of the respective techniques, such as the preparation of the SNOM tip or the tip-to-sample distance control.

SNOM tips produced by chemical etching of optical fibers are characterized by a large cone angle, thus a high transmission of 10^{-3}, with an aperture size of 70–100 nm [23][24].

For observations in liquid environment, a measuring cell has been developed that insures minimal degradation of the tip's mechanical properties to guarantee reliable distance control through shear-force measurements in liquid environment: lateral forces as small as 650 pN can be measured in water, allowing the near field above very soft samples to be probed [25].

Near-Field Optics at the Institute of Physics, University of Basel

Super-Resolution Imaging with Polarization Contrast

Polarization, like many other terms familiar from our knowledge of classical optics, requires reconsideration in NFO. The electric field next to a small circular aperture, illuminated with plane-polarized light, *e.g.*, resembles the superposition of a magnetic and an electric radiating dipole. The angular distribution of the radiation emerging from the probe/sample interaction region hence depends strongly on the state of polarization of the incident light.

The angular and polarization dependence of the light radiated from the probe/sample region was recently studied using a SNOM developed specifically for polarization-contrast microscopy [12][16]. Portions of the forbidden light were detected under different azimuth angles for given linear polarization states. The results obtain confirm predictions based on numerical simulations for the first time [26].

Polarization-contrast SNOM imaging is demonstrated in *Fig. 8*. The thin liquid-crystal polymer film imaged consists of areas having different molecular orientations. The resulting changes in birefringence are clearly visible in the image. The polarization of the illuminating light was kept constant during scanning. In order to determine both amplitude and orientation of, *e.g.*, a transition dipole moment on a

surface, a polarization-modulation scheme is better suited [27]. In this case the state of polarization of the illuminating light is continuously modulated. Modulation of the state of polarization allows optical activity, such as *Faraday* rotation on thin magnetic films [28], to be imaged.

Super-Resolution Fluorescence Imaging

A very promising avenue of SNOM, in particular for life sciences, is superresolution fluorescence imaging. This is exemplified in *Fig. 9*, which shows the surface of a glass slide onto which the fluorescence dye rhodamine-6G (R-6G) was deposited at low concentration. The topographic image shows the flat glass-slide surface only. The fluorescence image (*Fig. 9, b*) was recorded simultaneously using the aperture probe tip as a quasi-point light source to locally excite the dye molecules. The fluorescence photons were collected below the transparent sample with a high-resolution confocal optical microscope. The spatial resolution in the optical image is clearly better than diffraction limited. Additional experiments show that the isolated bright spots in this image are most likely caused by the emission from isolated single dye molecules.

Fig. 10 demonstrates how isolated dye molecules can serve as local optical probes for studying the rigidity of a thin (30 nm) polymer film (polyvinylbutyral) at ambient temperature. Here, the dye molecules are embedded between the backbones of the polymer molecules forming the film. The lateral displacement of the fluorescence spots in the sequence of images (the time lag between images is 14 min) is caused by diffusion of individual fluorescing molecules. This is summarized in the final graph, where the trajectories of all fluorescence spots of this series are plotted. The diffusion constants obtained from such experiments is on the order of 10^{-15} cm^2/s [30]. Such low diffusion constants are difficult to measure with a classical microscope.

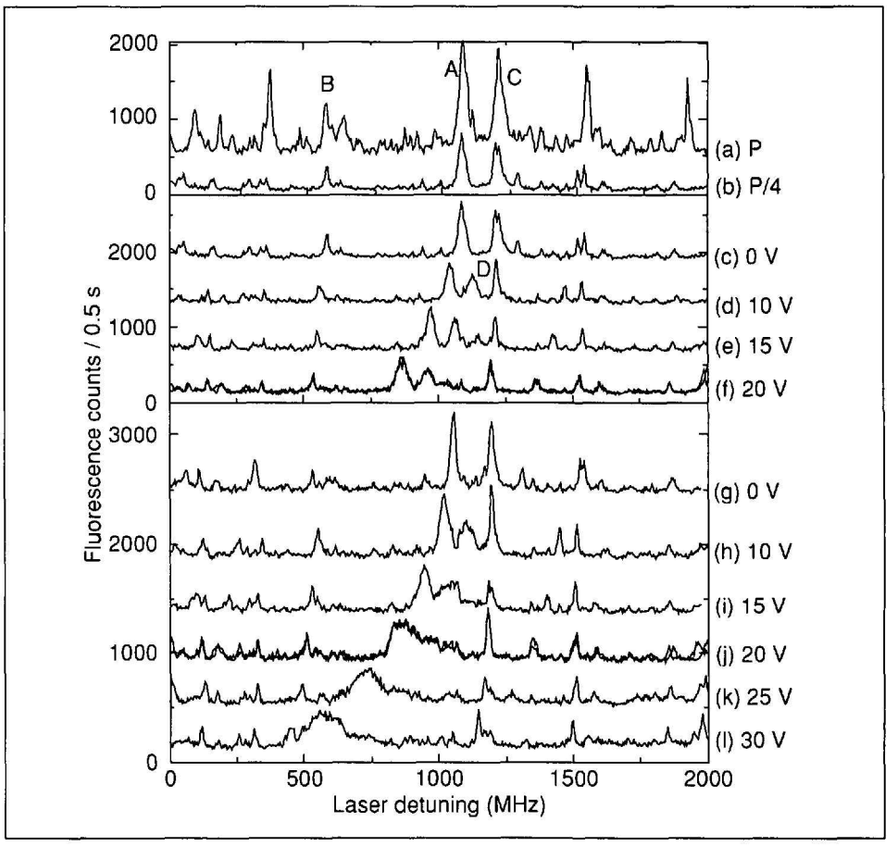

Fig. 11. *Excitation spectra showing three methods of identifying molecules close to the tip.* Upper panel: saturation method; spectra recorded with (a) 100 μW, and (b) 25 μW. Middle panel: static *Stark* shift method, traces labeled by the voltage applied to the optical probe. Bottom panel: *Stark* shift according to the lateral vibration method, traces labeled by the voltage applied to the optical probe. Zero detuning = 592.067 nm. From [31].

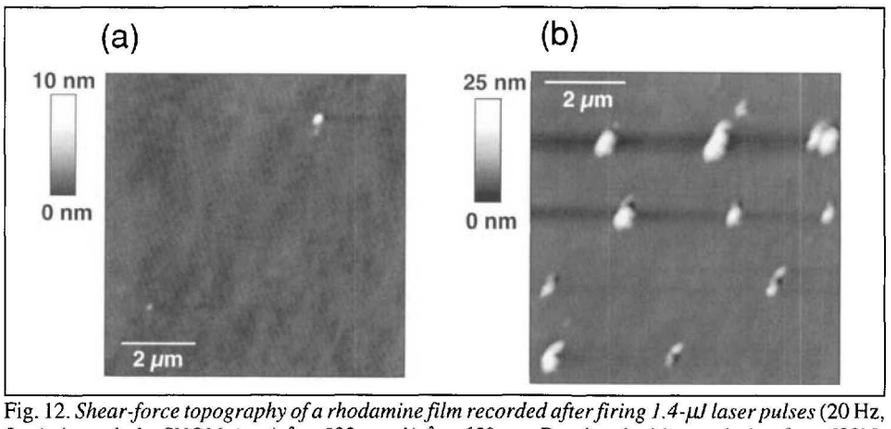

Fig. 12. *Shear-force topography of a rhodamine film recorded after firing 1.4-μJ laser pulses* (20 Hz, 5 ns) *through the SNOM tip. a)* λ = 532 nm, *b)* λ = 650 nm. Reprinted with permission from [32b]. Copyright 1997 American Chemical Society.

Near-Field Optics at ETH-Zürich

Single-Molecule Spectroscopy (SMS) and Microscopy at Cryogenic Temperatures

Molecules at cryogenic temperatures have a very high photo-stability as compared to room temperature: A molecule at 1.7 K may generally undergo as many as 10^{15} excitation cycles until it bleaches. A molecule at room temperature typically survives 10^5–10^8 excitations. As the width of the zero-phonon line (ZPL) at low temperature is only a few tens of MHz, the peak absorption cross section becomes extremely large. A molecular transition can, therefore, be saturated with moderate laser power. Furthermore, width and center frequency of ZPLs are extremely sensitive to the local nano-environment of the individual molecules. Such molecules can hence be viewed as the ultimate local probes.

The spectral selectivity of ZPL transitions is exploited for the study of low-temperature dynamics in solids at the Laboratory of Physical Chemistry. The absorption line of an ensemble of fluorescent molecules in a solid matrix is inhomogeneously broadened owing to the different nano-environments of the individual chromophores. If the frequency of a focussed narrow-band laser is tuned appropriately to a wing of such a line, only one molecule may be in resonance for a given setting. The position of such isolated mol-

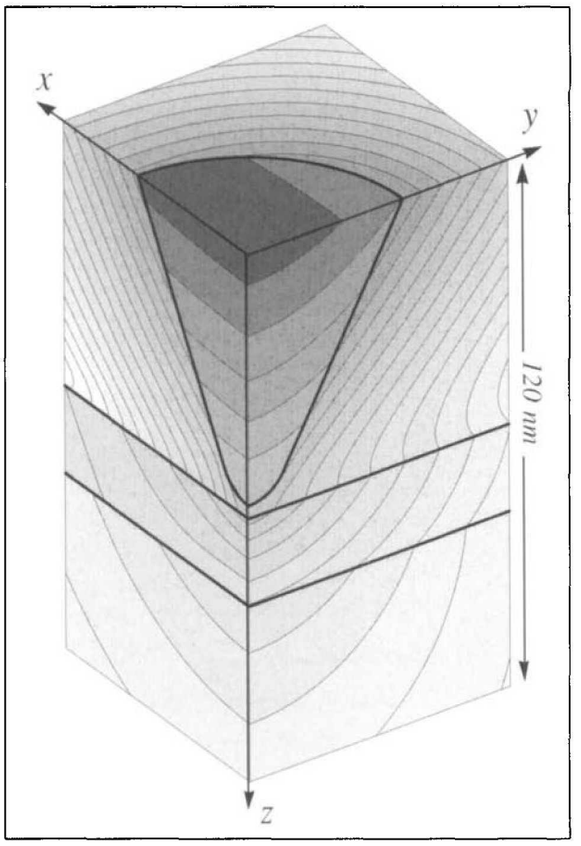

Fig. 13. *Contour lines of constant* $|\vec{E}|^2$ *on three perpendicular planes through the center of a SNOM probe.* From [34].

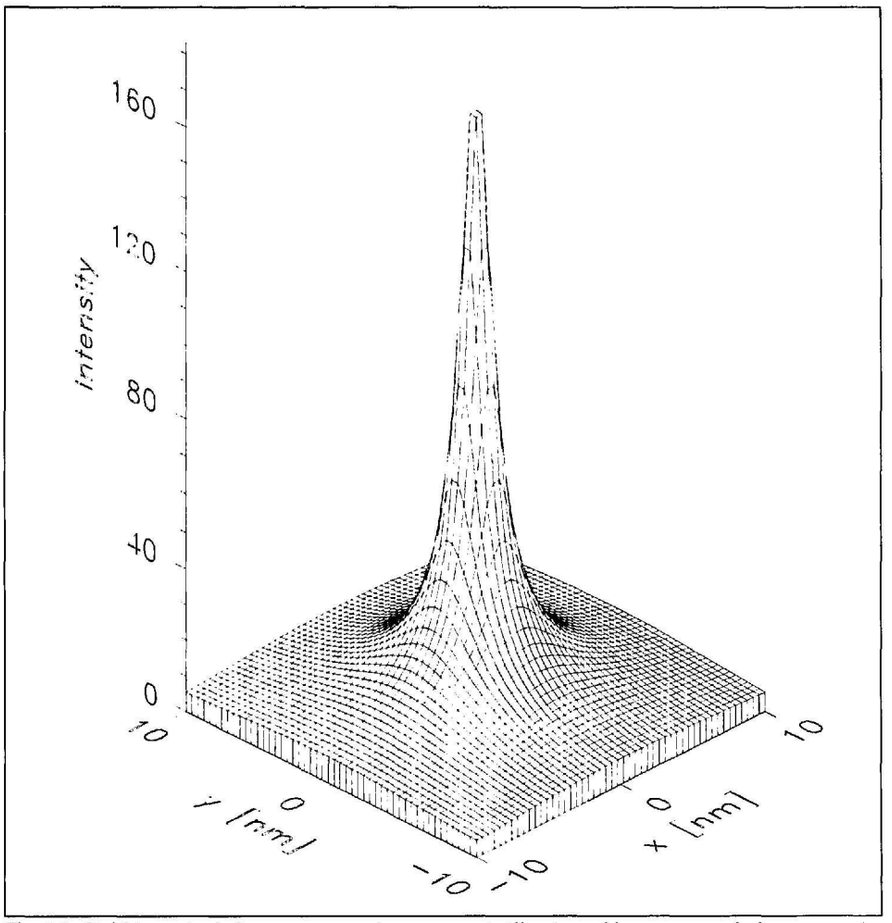

Fig. 14. *Field intensity below a nanometric tungsten tip illuminated by an external plane wave.* An enhancement factor of more than 180 times the incident field intensity is observed. From [37].

ecules in a matrix can be recorded with a conventional optical microscope if the molecules are spaced sufficiently far apart [29].

SNOM has the potential to drastically enhance the spatial resolution of SMS without sacrificing spectral sensitivity. Moreover, it introduces a number of new experimental opportunities. The distance of a molecule from the light-emitting optical probe can be estimated, *e.g.*, from the saturation properties of the molecular emission peaks [31]. This is illustrated in *Fig. 11*. Features A, B, and C in trace (a) are broadened apparently because of the large irradiance by the nearby optical probe. With decreasing intensity (trace (b)), these features do not decrease in proportion, in contrast to the other peaks apparently generated by more distant molecules. A striking novel feature of this combined SMS/SNOM experiments is the possibility to study the interaction of individual molecules with local electric fields. For this purpose, it is sufficient to apply a voltage to the metal coating of the optical probe. The influence of the dc *Stark* effect on the absorption spectrum is demonstrated by traces (c)–(f) of *Fig. 11*. Feature A, obviously closest to the rim of the aperture probe, shows the expected quadratic shift, while many other features remain unchanged.

In traces (g)–(l) of *Fig. 11*, the influence of a small amplitude vibration of the optical probe with applied electric field on the spectrum is presented. The broadening of the individual lines is proportional to the gradient of the electric field at the position of the respective molecules.

Experiments are under way to further study the nanoscopic interaction of single molecules with nearby scanned probes. They can help to gain a better understanding of the dynamic behavior of single molecules in crystalline hosts and may also lead to novel mircroscopic imaging techniques.

Photo-Physics/-Chemistry at the Nanometer Scale

For NFO desorption and ablation experiments [17][32] at the Laboratory for Organic Chemistry, pulsed laser light from a Nd:YAG pumped optical parametric oscillator with a pulse width of 3–6 ns and variable wavelength was coupled into the multimode optical fiber probe of a SNOM. *Fig. 12, a* shows the topography of a thin dye film after firing light pulses at a fixed repetition rate of 20 Hz through the nanometer-sized probe aperture. A smooth surface and no ablation were observed for the off-resonance wavelenght of $\lambda = 650$ nm.

However, well-defined craters were created by light with $\lambda = 532$ nm (*Fig. 12, b*), which is strongly absorbed by the dye.

Crater formation by light at the resonant wavelength is evidence of an optical ablation mechanism, either photochemical or photothermal. Depressions with a diameter (FWHM) as small as 85 nm and a depth of 5 nm could be produced. The protrusions visible in *Fig. 12, b* may be interpreted as ablated molecules that were redeposited on the substrate. The amount of redeposited material around the craters varies strongly, owing to shot-to-shot variations of the laser pulse energy, amplified by a nonlinear irradiance dependence of the ablation yield. The redeposition apparently occurs in a preferred direction, probably due to an asymmetric tip shape.

Computational NFO

The Institute for Field Theory and Microwave Electronics (IFH) has a well-founded experience in computational electronics. On this basis, specific models for the theoretical investigation of NFO problems were developed in the past years. Our research addresses several aspects of SNOM, such as the confinement of light by a near-field probe [33][34], the contrast mechanisms and the relation between image and object [35], as well as the fluorescence of single molecules trapped at a near-field probe apex [36].

Figs. 13 and *14* illustrate two complementary ways of achieving the light confinement required for a good SNOM probe: *Fig. 13* shows the propagation of light through the end of an a-SNOM probe. The glass core is covered with a continuous high-reflectivity aluminum coating. The metal film is reduced in thickness at the apex. The resulting semi-transparent zone acts as aperture [34].

In *Fig. 14*, a plane metallic tip is illuminated by an external field. Owing to the small radius of curvature, strong optical fields appear at the tip apex. These fields can easily be tuned by changing the external parameters such as the polarization or the angle of incidence of the external field [37].

Field determinations of the type shown require intense computation but are instrumental for the design of improved SNOM probes and optimization of a given scheme. They help to focus the respective experimental efforts on the most promising schemes, an aspect that is particularly important in view of the required nanometer-scale processing and manipulation, which are not easy to control.

Summary

SNOM provides optical images with a linear resolution up to ten times better than that of conventional optical microscopes. The technique still is at an experimental stage, mainly because of the difficulties associated with the preparation of near-field optical probes. With increasing mastery of nanometer-scale structuring, progress towards routine operation and towards further improvements in resolution may be expected. The research groups in Switzerland are in a position to contribute significantly to the future development of near-field optical techniques.

Received: August 28, 1997

[1] H. Heinzelmann, T. Huser, T. Lacoste, H.-J. Güntherodt, D.W. Pohl, B. Hecht, L. Novotny, O.J.F. Martin, C. Hafner, H. Baggenstos, U.P. Wild, A. Renn, *Opt. Eng.* **1995**, *34*, 2441.
[2] D.W. Pohl, W. Denk, M. Lanz, *Appl. Phys. Lett.* **1984** *44*, 651.
[3] D.W. Pohl, W. Denk, U. Dürig, in 'Micron and Submicron Integrated Circuit Metrology', Ed. K.M. Monahan, *Proc. SPIE* **1985**, *565*, 56.
[4] U. Dürig, D.W. Pohl, F. Rohner, *J. Appl. Phys.* **1986**, *59*, 3318.
[5] E. Betzig, A. Lewis, A. Harootunian, M. Isaacson, E. Kratschmer, *Biophys. J.* **1986**, *49*, 269.
[6] U.C. Fischer, U.T. Dürig, D.W. Pohl, *Appl. Phys. Lett.* **1988**, *52*, 249.
[7] E. Betzig, in 'Near Field Optics', Eds. D.W. Pohl, and D. Courjon, Kluwer, Dordrecht, 1993, NATO ASI Series E: Applied Sciences, Vol. 242. pp. 7–15.
[8] B. Hecht, H. Bielefeldt, Y. Inouye, D.W. Pohl, L. Novotny, *J. Appl. Phys.* **1997**, *81*, 2492.
[9] B. Hecht, H. Heinzelmann, D.W. Pohl, *Ultramicroscopy* **1995**, *57*, 228.
[10] H. Heinzelmann, B. Hecht, L. Novotny, D.W. Pohl, *J. Microsc.* **1994**, *177*, 115.
[11] A.J. Meixner, M.A. Bopp, G. Tarrach, *Appl. Opt.* **1994**, *33*, 7995.
[12] T. Lacoste, T. Huser, H. Heinzelmann, H.-J. Güntherodt, in 'Photons and Local Probes', Eds. O. Marti and R. Möller, Kluwer, Dordrecht, 1995, NATO ASI Series E: Applied Sciences, Vol. 300, pp. 123–132.
[13] B. Hecht, D.W. Pohl, H. Heinzelmann, L. Novotny, *Ultramicroscopy* **1995**, *61*, 99.
[14] G. Tarrach, M.A. Bopp, D. Zeisel, A.J. Meixner, *Rev. Sci. Instrum.* **1995**, *66*, 3569.
[15] B. Hecht, 'Forbidden Light Scanning Near-Field Optical Microscopy', Ph.D. thesis, University of Basel, Hartung-Gorre Verlag, Konstanz, 1996.
[16] H. Heinzelmann, T. Lacoste, T. Huser, H.-J. Güntherodt, B. Hecht, D.W. Pohl, *Thin Solid Films* **1996**, *273*, 149.
[17] D. Zeisel, B. Dutoit, V. Deckert, T. Roth, R. Zenobi, *Anal. Chem.* **1997**, *69*, 749.
[18] U. Keller, B. Nechay, U. Siegner, 'Ultrafast local probes for semiconductor spectroscopy' (1997), see: http://www.rereth.ethz.ch/phys/quantenelektronik/keller/pj.10.html.
[19] D.W. Pohl, U.C. Fischer, U.T. Dürig, in 'Scanning Microscopy Technologies and Applications', Ed. E.C. Teague, *Proc. SPIE* **1988**, *897*, 84.
[20] B. Hecht, H. Bielefeldt, L. Novotny, Y. Inouye, D.W. Pohl, *Phys. Rev. Lett.* **1996**, *77*, 1889.
[21] U.C. Fischer, D.W. Pohl, *Phys. Rev. Lett.* **1989**, *62*, 458.
[22] P. Hofmann, B. Dutoit, R.P. Salathe, *Ultramicroscopy* **1995**, *61*, 165.
[23] M. Pfeffer, P. Lambelet, F. Marquis-Weible, *Rev. Sci. Instrum.* **1997**, (to be published).
[24] A. Sayah, C. Philipona, P. Lambelet, M. Pfeffer, F. Marquis-Weible, *Ultramicroscopy* **1997**, (to be published).
[25] P. Lambelet, M. Pfeffer, A. Sayah, F. Marquis-Weible, *Ultramicroscopy* **1997**, (to be published).
[26] L. Novotny, D.W. Pohl, P. Regli, *Ultramicroscopy* **1995**, *57*, 180.
[27] T. Lacoste, T. Huser, R. Prioli, H. Heizelmann, *Ultramicroscopy* **1997**, (to be published).
[28] T. Lacoste, T. Huser, H. Heinzelmann, *Z. Phys. B* **1997**, (to be published).
[29] J. Jasny, J. Sepiol, T. Irngartinger, M. Traber, A. Renn, U.P. Wild, *Rev. Sci., Instrum.* **1996**, *67*, 1425.
[30] M.A. Bopp, A.J. Meixner, G. Tarrach, I. Zschokke-Gränacher, L. Novotny, *Chem. Phys. Lett.* **1996**, *263*, 721.
[31] W.E. Moerner, T. Plakhotnik, T. Irngartinger, U.P. Wild, D.W. Pohl, B. Hecht, *Phys. Rev. Lett.* **1994**, *73*, 2764.
[32] a) D. Zeisel, S. Nettesheim, B. Dutoit, R. Zenobi, *Appl. Phys. Lett.* **1996**, *68*, 2941; b) B. Dutoit, D. Zeisel, V. Deckert, R. Zenobi, *J. Phys. Chem. B* **1997**, *101*, 6955.
[33] L. Novotny, C. Hafner, *Phys. Rev. E* **1994**, *50*, 4094.
[34] L. Novotny, D.W. Pohl, B. Hecht, *Opt. Lett.* **1995**, *20*, 970.
[35] O.J.F. Martin, C. Girard, A. Dereux, *J. Opt. Soc. Am. A* **1996**, *13*, 1801.
[36] C. Girard, O.J.F. Martin, A. Dereux, *Phys. Rev. Lett.* **1995**, *75*, 3098.
[37] O.J.F. Martin, C. Girard, *Appl. Phys. Lett.* **1996**, *70*, 705.